Precoder Distribution and Adaptive Codebook in Wideband Precoding

Hang Long, Kyeong Jin Kim, Wei Xiang, Jing Wang, Yuanan Liu, and Wenbo Wang

Based on wideband precoding (WBP) in the multiple-input multiple-output orthogonal frequency division multiplexing system, an adaptive nonuniform codebook is presented in this paper. The relationship between the precoder distribution and spatial correlation is analyzed at first. A closed-form expression based on overlapped isosceles triangles is proposed as an approximation of the precoder distribution. Then, the adaptive codebook design is derived with the approximate distribution to minimize quantization errors. The capacity and bit error rate performance demonstrate that the adaptive codebook with WBP outperforms the conventional fixed uniform codebook.

Keywords: MIMO, OFDM, precoding, spatial correlation, quantization.

Manuscript received Jan. 28, 2012; revised May 18, 2012; accepted June 1, 2012.

This work was supported by the National Science Foundation for Post-doctoral Scientists of China (20110490329) and National Basic Research Program of China (973 Program) (2012CB316005).

Hang Long (phone: +86 10 6119 8066-4, lhrzrzlh@bupt.edu.cn) is with the School of Electronics Engineering, Beijing University of Posts & Telecommunications, and also with the the Wireless Signal Processing and Network Lab., Key Laboratory of Universal Wireless Communication, Ministry of Education, Beijing University of Posts & Telecommunications, Beijing, China.

Kyeong Jin Kim (kyeong.j.kim@hotmail.com) was with the UWB Wireless Communications Research Center, Inha University, Incheon, Rep. of Korea, and now is with the Mitsubishi Electric Research Laboratories, Boston, MA, USA.

Wei Xiang (wei.xiang@usq.edu.au) is with the Faculty of Engineering and Surveying, University of Southern Queensland, Toowoomba, Australia.

Jing Wang (wjwendy1989@gmail.com) and Wenbo Wang (wbwang@bupt.edu.cn) are with the Wireless Signal Processing and Network Lab., Key Laboratory of Universal Wireless Communication, Ministry of Education, Beijing University of Posts & Telecommunications, Beijing, China.

Yuanan Liu (yuliu@bupt.edu.cn) is with the School of Electronics Engineering, Beijing University of Posts & Telecommunications, Beijing, China.

http://dx.doi.org/10.4218/etrij.12.0112.0072

I. Introduction

Multiple-input multiple-output (MIMO) technology has been proven to be able to tremendously improve the spectral efficiency in rich scattering environments [1]. The orthogonal frequency division multiplexing (OFDM) technique has been in widespread use in high data rate wireless communication systems due to its high spectrum efficiency and tolerance of inter-symbol interference [2], [3]. Hence, MIMO-OFDM systems have attracted significant worldwide research efforts [4].

In MIMO systems, the precoding technique is able to enhance the system reliability and capacity [5]. Conventional precoding schemes are usually designed for narrowband MIMO systems with flat fading, which are not suitable for MIMO-OFDM systems with frequency-selective fading. A wideband precoding (WBP) scheme is presented in [6] and [7], where only one precoder is used for all the subcarriers in the MIMO-OFDM system. The precoder is obtained from a subcarrier independent channel matrix constructed through the temporal channel vectors. The channel state information feedback overhead can be significantly reduced especially if the number of subcarriers is large. Based on the work in [6] and [7], the relationship between the subcarrier independent channel matrix and the temporal/frequency channel matrices is investigated and an improved WBP scheme is proposed for arbitrary subcarrier grouping in [8]. The idea of WBP is extended to the MIMO-OFDM cooperative system with a relay node in [9]. However, the precoder distribution for WBP is still an open problem, which is important for the use of WBP in the system with limited feedback.

On the other hand, the codebook-based precoding technique is suitable for practical implementation with reduced feedback

overhead [10]-[12]. For codebook-based precoding, the quantization of a potential precoder is a challenging problem in the codebook design. For independent and identically distributed (i.i.d.) MIMO channels, the conventional precoder (right singular vectors of the channel matrix) is isotropically distributed in the set of unitary matrices [12]-[14]. Therefore, the codebook design is usually considered to be a classical Grassmanian packing problem, as in [11] and [12]. In practical applications, uniform quantization in the set of unitary matrices is simple and useful for the codebook design. The precoder distribution under spatially correlated channels is analyzed in [14], and an adaptive nonuniform codebook design is proposed for MIMO systems, where the codebook is designed in consideration of the correlation coefficient.

In this paper, based on WBP in MIMO-OFDM systems under spatially correlated channels, the precoder distribution is analyzed and found to be affected by the spatial correlation coefficients of all the resolvable taps of the channel, which is different from the narrowband MIMO system. Then, the distribution is approximated by multiple overlapped isosceles triangles. An adaptive nonuniform codebook is designed for WBP accordingly. Simulation results demonstrate that the proposed adaptive codebook is able to reduce quantization errors and outperforms the fixed uniform codebook in system capacity and reliability.

The remainder of this paper is organized as follows. The system model is described in section II. The WBP scheme is reviewed in section III. The precoder distribution is analyzed and the approximate expressions are presented in section IV. Accordingly, the adaptive codebook is designed in section V. Simulation results are given in section VI. Finally, section VII concludes this paper.

Notation. The transpose and conjugate-transpose of matrix $\mathbf{A}$ are denoted by $\mathbf{A}^{\mathrm{T}}$ and $\mathbf{A}^{\mathrm{H}}$, respectively. The $n\times n$ identity matrix and $m\times n$ all-zero matrix are denoted by $\mathbf{I}_n$ and $\mathbf{O}_{m,n}$, respectively. Mathematical expectation is denoted by $E(\cdot)$, and $\otimes$ denotes the Kronecker product of two matrices. The vector space of all $m\times n$ complex matrices is denoted by $\mathbb{C}^{m\times n}$. The largest integral smaller than x is denoted by $\lfloor x \rfloor$.

II. System Model

We consider the MIMO-OFDM system with the discrete Fourier transform (DFT) of size N and L input spatial streams. Equipped at the transmitter and receiver are N_{T} and N_{R} antennas, respectively. The maximum path delay is assumed to be shorter than the length of the cyclic prefix (CP), $N_{\mathrm{T}} \geq L$, and $N_{\mathrm{R}} \geq L$.

The equivalent MIMO system over the n-th subcarrier can be written as

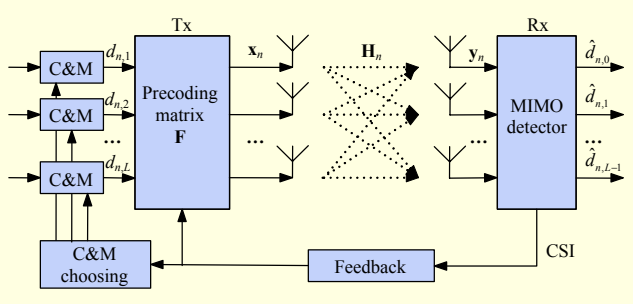

Fig. 1. Illustration of MIMO system over n-th subcarrier.

$$\mathbf{y}_n = \mathbf{H}_n \mathbf{x}_n + \mathbf{z}_n, \quad n \in \{0,1,\ldots,N-1\}, \tag{1}$$

where $\mathbf{x}_n \in \mathbb{C}^{N_{\mathrm{T}}\times 1}$ and $\mathbf{y}_n \in \mathbb{C}^{N_{\mathrm{R}}\times 1}$ are the transmitted and received signal vectors, respectively, $\mathbf{z}_n$ is the additive white Gaussian noise at the receiver $\mathbf{z}_n \sim \mathcal{CN}(\mathbf{0}_{N_{\mathrm{R}},1}, \sigma^2 \mathbf{I}_{N_{\mathrm{R}}})$, and $\mathbf{H}_n \in \mathbb{C}^{N_{\mathrm{R}}\times N_{\mathrm{T}}}$ is the MIMO channel matrix over the n-th subcarrier.

The equivalent MIMO system is illustrated in Fig. 1, where $d_{n,i}$ is the symbol of the i-th spatial data stream to be sent over the n-th subcarrier, $i \in \{1, 2,\ldots, L\}$. That is, $\mathbf{d}_n = [\, d_{n,1}, d_{n,2},\ldots, d_{n,L}]^{\mathrm{T}}$ is the data vector before precoding.

$$E(\mathbf{d}_n \mathbf{d}_{n'}^{\mathrm{H}}) = \begin{cases} 1/L \cdot \mathbf{I}_L & n = n', \\ \mathbf{0}_{L,L} & n \neq n'. \end{cases} \tag{2}$$

The precoder over all the N subcarriers is $\mathbf{F}$, and $\mathbf{x}_n = \mathbf{F}\mathbf{d}_n$.

As described in [6]-[8], $\mathbf{H}_n$ can be denoted by the temporal channel $h_l^{p,q}$, which is the temporal channel of the l-th tap between the p-th transmit and the q-th receive antennas, where $l \in \{1, 2,\ldots, N_f\}$, $p \in \{1, 2,\ldots, N_{\mathrm{T}}\}$, and $q \in \{1, 2,\ldots, N_{\mathrm{R}}\}$. The channel order N_f is determined as

$$N_f = \lfloor \tau_{\max} / \Delta t \rfloor + 1, \tag{3}$$

where $\tau_{\max}$ is the maximum path delay and Δt is the temporal sampling interval. The temporal channel vector between the p-th transmit and the q-th receive antennas is given by

$$\mathbf{h}^{p,q} = [h_1^{p,q}, h_2^{p,q}, \ldots, h_{N_f}^{p,q}]^{\mathrm{T}}. \tag{4}$$

Using (4), $\mathbf{H}_n$ can be expressed in terms of $\mathbf{h}^{p,q}$ [6], [7]:

$$\mathbf{H}_n = \begin{bmatrix} \mathbf{w}_n^{\mathrm{T}} \mathbf{h}^{1,1} & \cdots & \mathbf{w}_n^{\mathrm{T}} \mathbf{h}^{N_{\mathrm{T}},1} \\ \vdots & \ddots & \vdots \\ \mathbf{w}_n^{\mathrm{T}} \mathbf{h}^{1,N_{\mathrm{R}}} & \cdots & \mathbf{w}_n^{\mathrm{T}} \mathbf{h}^{N_{\mathrm{T}},N_{\mathrm{R}}} \end{bmatrix}, \tag{5}$$

where

$$\mathbf{w}_n = [1, \mathrm{e}^{-j\cdot 2\pi n/N}, \mathrm{e}^{-j\cdot 2\pi n\cdot 2/N}, \ldots, \mathrm{e}^{-j\cdot 2\pi n\cdot (N_f-1)/N}]^{\mathrm{T}}. \tag{6}$$

III. Wideband Precoding Review

In the WBP scheme [6], [7], only one precoder is used for all

the subcarriers. Equation (5) can be rewritten as

$$\mathbf{H}_n = (\mathbf{I}_{N_R} \otimes \mathbf{w}_n^{\mathrm{T}})\mathbf{H}, \tag{7}$$

where

$$\mathbf{H} = \begin{bmatrix} \mathbf{h}^{1,1} & \cdots & \mathbf{h}^{N_{\mathrm{T}},1} \\ \vdots & \ddots & \vdots \\ \mathbf{h}^{1,N_{\mathrm{R}}} & \cdots & \mathbf{h}^{N_{\mathrm{T}},N_{\mathrm{R}}} \end{bmatrix} \tag{8}$$

is the subcarrier independent channel matrix. The singular value decomposition of $\mathbf{H}$ is obtained at the receiver as

$$\mathbf{H} = \mathbf{U}\boldsymbol{\Sigma}\mathbf{V}^{\mathrm{H}}. \tag{9}$$

The first L right singular vectors are used as the precoder:

$$\mathbf{F} = \mathbf{V}[\mathbf{I}_L, \mathbf{0}_{L,N_{\mathrm{T}}-L}]^{\mathrm{T}}, n \in \{0,1,...,N-1\}. \tag{10}$$

The relationship between $\mathbf{H}$ and the temporal/frequency MIMO channel matrices is given in [8]. The temporal MIMO channel matrix of the i-th tap is constructed by $\{h_l^{p,q}\}$ as

$$\mathbf{H}_i^{(t)} = \begin{bmatrix} h_i^{1,1} & \cdots & h_i^{N_{\mathrm{T}},1} \\ \vdots & \ddots & \vdots \\ h_i^{1,N_{\mathrm{R}}} & \cdots & h_i^{N_{\mathrm{T}},N_{\mathrm{R}}} \end{bmatrix}, i \in \{1,2,...,N_f\}. \tag{11}$$

It is summarized in [8] that

$$\mathbf{H}^{\mathrm{H}}\mathbf{H} = \sum_{i=0}^{N_f-1} [\mathbf{H}_i^{(t)}]^{\mathrm{H}} \mathbf{H}_i^{(t)}. \tag{12}$$

That is, the covariance matrix of the subcarrier independent channel is the sum of the covariance matrices of the temporal MIMO channel matrices [8].

Based on WBP reviewed previously, codebook-based WBP under spatially correlated channels is investigated below. The major contributions of this paper can be summarized as follows:

1) The precoder distributions of WBP under correlated channels are given under various channel assumptions. Then, a unified approximate expression of the precoder distribution is presented in section IV. The proposed approximate expression can also be used for narrowband precoders.

2) An adaptive codebook for WBP is designed in section V with the proposed approximate expressions in section IV. Simulation results in section VI demonstrate that the proposed adaptive codebook outperforms the conventional fixed codebook both in the bit error rate (BER) and the capacity.

IV. Precoder Distribution under Correlated Channel

The spatial correlation matrices of the i-th tap at the transmitter and receiver are defined as

$$E\{[\mathbf{H}_i^{(t)}]^{\mathrm{H}} \mathbf{H}_i^{(t)}\} = P_i \mathbf{R}_{\mathrm{T}i} \tag{13}$$

and

$$E\{\mathbf{H}_i^{(t)}[\mathbf{H}_i^{(t)}]^{\mathrm{H}}\} = P_i \mathbf{R}_{\mathrm{R}i}, \tag{14}$$

respectively. In (13) and (14), P_i is the average power of the i-th tap. According to [14], the receiver correlation matrix $\mathbf{R}_{\mathrm{R}i}$ does not affect the precoder distribution. Hence, it is assumed in the sequel that

$$\mathbf{R}_{\mathrm{R}i} = \mathbf{I}_{N_{\mathrm{R}}}, \forall i \in \{1,2,...,N_f\}. \tag{15}$$

For brevity of exposition, it is assumed that N_{T}=2, so that the spatial correlation matrix at the transmitter can be written as

$$\mathbf{R}_{\mathrm{T}i} = \begin{bmatrix} 1 & \beta_i \\ \beta_i^* & 1 \end{bmatrix}, \beta_i = |\beta_i| e^{j\varphi_i}, \tag{16}$$

where β_i is the correlation coefficient at the transmitter of the i-th tap. As shown in (10), $\mathbf{F}$ is related to $\mathbf{V}$. A generalized expression of $\mathbf{V}$ is given as [14]

$$\mathbf{V} = \begin{bmatrix} \cos\theta_1 & \sin\theta_1 \\ \sin\theta_1 e^{j\theta_2} & \cos\theta_1 e^{j(\theta_2+\pi)} \end{bmatrix}, \theta_1 \in \left[0, \frac{\pi}{2}\right], \theta_2 \in [-\pi, \pi). \tag{17}$$

Here, $\mathbf{V}$ can be uniquely identified with θ_1 and θ_2. Thus, the precoder distribution is equivalent to the distribution of θ_1 and θ_2. The precoder distribution in the narrowband MIMO system can be found in [14], which is related to the correlation coefficient β. The distribution of θ_1 is not affected by the angle of β. The adaptive nonuniform codebook amounts to the adaptive quantization of θ_2 according to β [14]. Hence, we focus on the distribution of θ_2 in this study. It is also assumed that L=1. That is, the precoder is the first column of $\mathbf{V}$. The results in this study can be easily extended to the case of L=2.

1. Distribution of Right Singular Vector

If $|\beta_i| = 0$, $i \in \{1, 2, \ldots, N_f\}$, that is, under the i.i.d. fading channel, the precoder distribution is identical to that in the i.i.d. narrowband MIMO systems [12]-[15]. That is, $\mathbf{V}$ is isotropically distributed in the set of unitary matrices. This means that $\cos^2\theta_1$ and θ_2 are uniformly distributed in the intervals of [0, 1] and $[-\pi, \pi)$, respectively [14].

In narrowband precoding, the distribution center of θ_2 is related to the angle of the correlation coefficient [14]. We can also readily see that the distribution of the wideband precoder under the spatial correlated channel is related to φ_i.

A. Equal Correlation Coefficient for All Taps

In this case, the correlation coefficients of all the taps are assumed to be identical, that is, $\beta_i = \beta$, $\forall\, i \in \{1, 2, \ldots, N_f\}$. The precoder distributions are the same as those in narrowband MIMO systems. The probability density function (PDF) of θ_2, $p(\theta_2)$ is obtained with Monte Carlo simulations, which is plotted with the black line in Fig. 2. The relationship between β

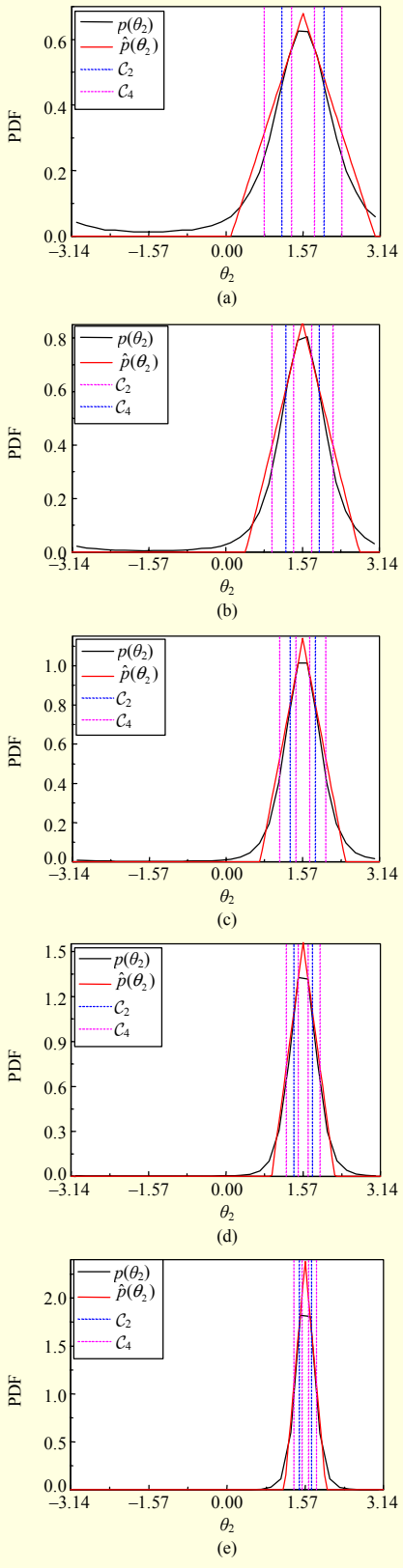

Fig. 2. Precoder distribution for (a) $\beta_i=\beta=0.5e^{j\pi/2}$, (b) $\beta_i=\beta=0.6e^{j\pi/2}$, (c) $\beta_i=\beta=0.7e^{j\pi/2}$, (d) $\beta_i=\beta=0.8e^{j\pi/2}$, and (e) $\beta_i=\beta=0.9e^{j\pi/2}$.

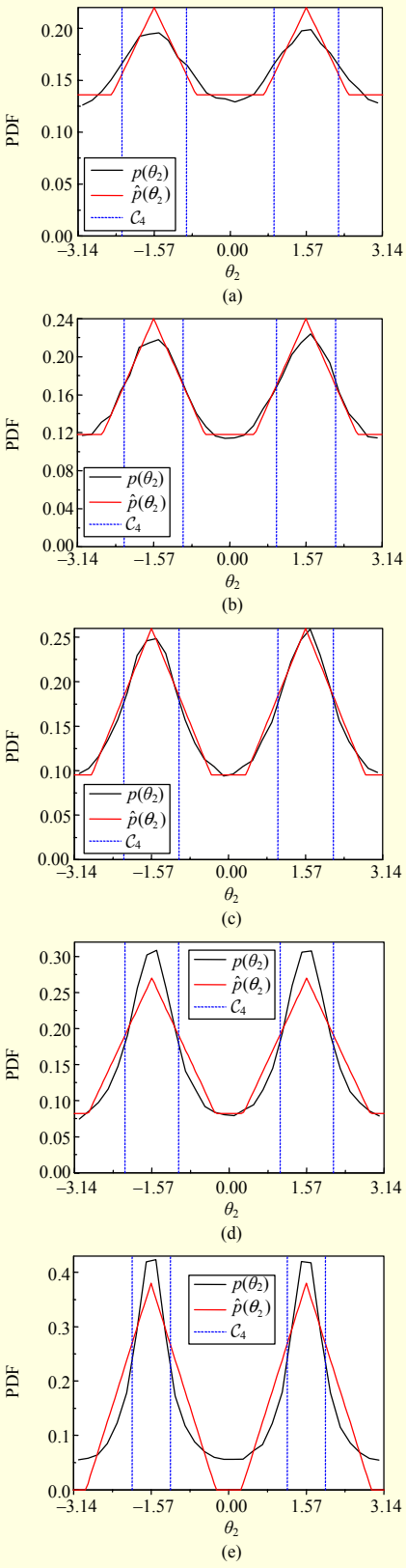

Fig. 3. Precoder distribution for $P_1=P_l=0.5$, $\varphi_1=-\pi/2$, $\varphi_l=\pi/2$: (a) $|\beta_1|=|\beta_l|=0.5$, (b) $|\beta_1|=|\beta_l|=0.6$, (c) $|\beta_1|=|\beta_l|=0.7$, (d) $|\beta_1|=|\beta_l|=0.8$, and (e) $|\beta_1|=|\beta_l|=0.9$.

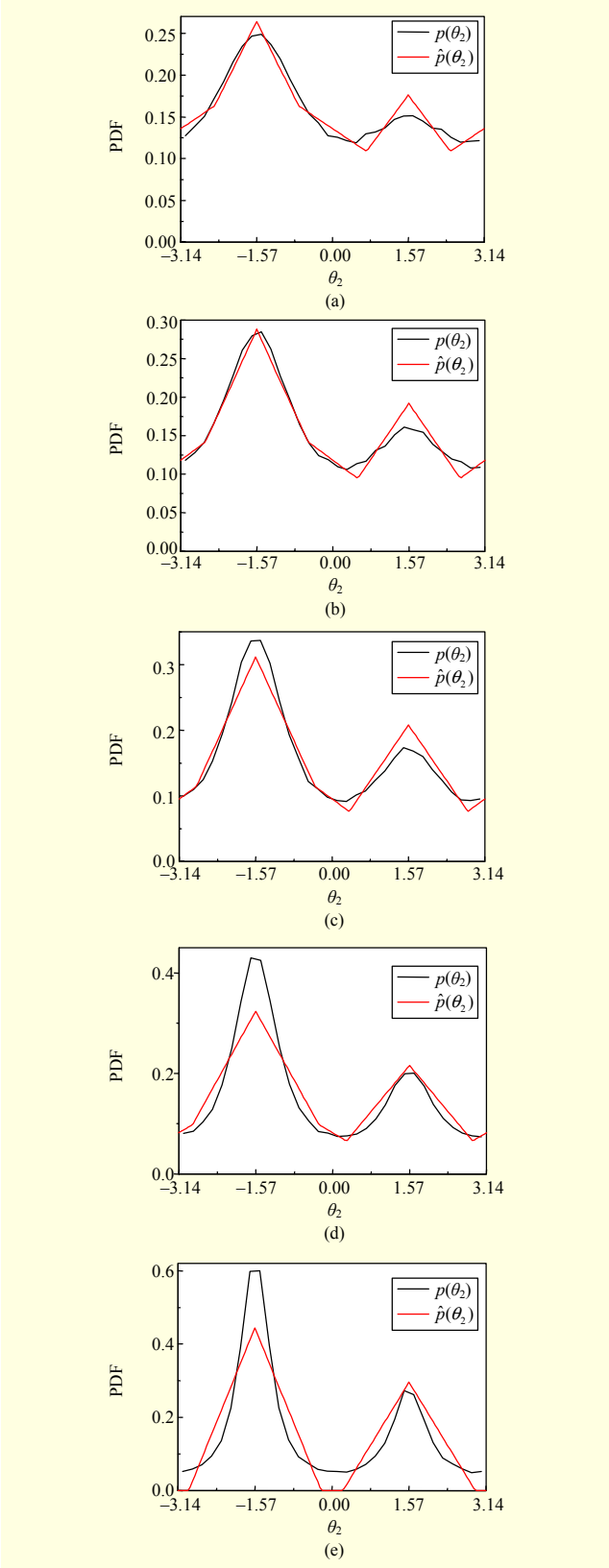

Fig. 4. Precoder distribution for P_1=0.6, P_l=0.4, φ_1=–π/2, and φ_l=π/2: (a) $|\beta_1|$=$|\beta_l|$=0.5, (b) $|\beta_1|$=$|\beta_l|$=0.6, (c) $|\beta_1|$=$|\beta_l|$=0.7, (d) $|\beta_1|$=$|\beta_l|$=0.8, and (e) $|\beta_1|$=$|\beta_l|$=0.9.

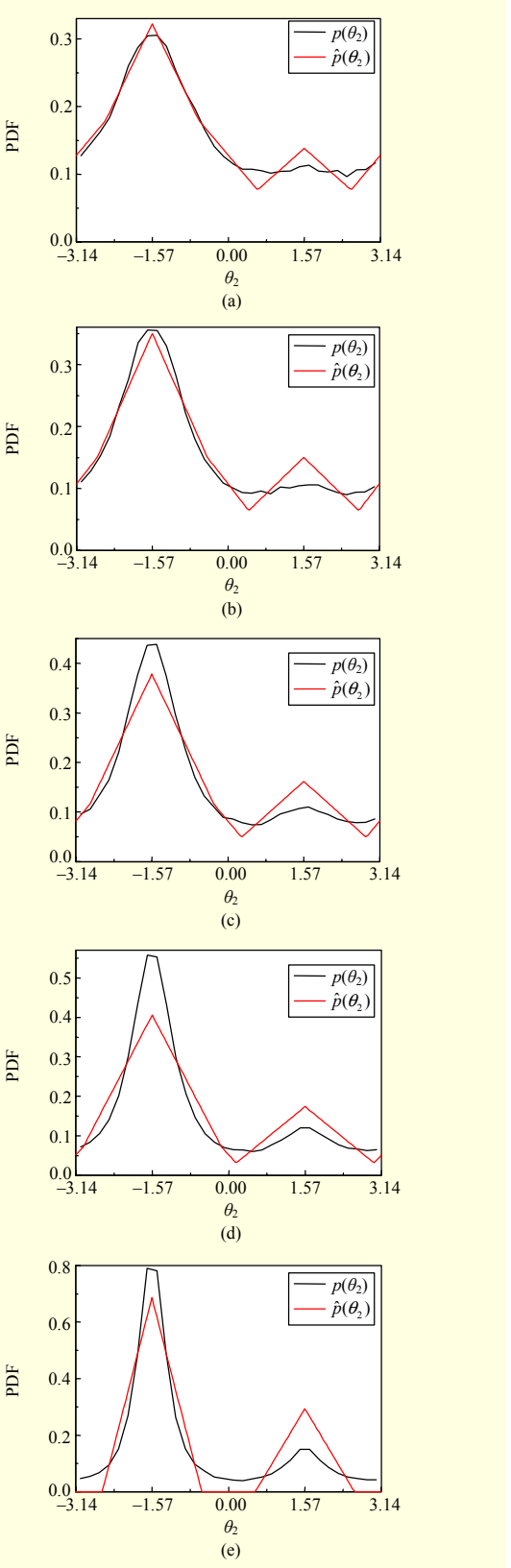

Fig. 5. Precoder distribution for P_1=0.7, P_l=0.3, φ_1=–π/2, and φ_l=π/2: (a) $|\beta_1|$=$|\beta_l|$=0.5, (b) $|\beta_1|$=$|\beta_l|$=0.6, (c) $|\beta_1|$=$|\beta_l|$=0.7, (d) $|\beta_1|$=$|\beta_l|$=0.8, and (e) $|\beta_1|$=$|\beta_l|$=0.9.

and $p(\theta_2)$ is similar to those relationships summarized in [14]: $p(\theta_2)$ is a symmetrical function of which the symmetrical axis is $\theta_2=\varphi$; the distribution of θ_2 is mainly near φ, and the variance of θ_2 decreases as $|\beta|$ increases.

B. Different Correlation Coefficients for All Taps

As shown in (12), **H** and **V** are independent of the delay of all the taps and related to power P_i and correlation coefficient β_i of each tap. For our investigation, a two-tap channel with $P_1>0$, $P_l>0$, $P_{l'}=0$, $1<l$, $l'\le N_f$, $l'\ne l$, and $P_1+P_l=1$ is considered.

a. Equal Power Case

The precoder distributions with $P_1=P_l=0.5$ are shown in Fig. 3 with the black line. As can be seen from the figures, two peaks of $p(\theta_2)$ exist near $\varphi_1=-\pi/2$ and $\varphi_l=\pi/2$. The variance of θ_2 around φ_1 and φ_l also decreases with the increase of $|\beta_1|$ and $|\beta_l|$. It is easy to know the envelope of the PDFs under other assumptions of φ_1 and φ_l.

b. Nonequal Power Case

Different powers at the taps are considered for the cases of $P_1=0.6$ and $P_1=0.7$. The precoder distributions are given in Figs. 4 and 5. The two peaks of the PDF still exist, and the one around $\varphi_1=-\pi/2$ is higher and wider than the one around $\varphi_l=\pi/2$.

2. Approximation of Precoder Distribution

Figures 2 through 5 show some characteristics of $p(\theta_2)$ under four different scenarios.

- The peaks are related to the channel taps.
- The locations of the peaks are equal to φ_i.
- The height and the area under each peak are related to P_i, and the area under the peak increases as P_i increases.
- The height of each peak is also related to $|\beta_i|$.

The envelope of each peak of the PDF can be represented by an isosceles triangle, as shown in Figs. 2 through 5. As a result, we can use the following isosceles triangle function to approximate the distribution related to each tap:

$$f_i(\theta_2)=2P_i\begin{cases}2h^2(\theta_2-\varphi_i)+h, \theta_2\in[\varphi_i-1/(2h),\varphi_i]\\ -2h^2(\theta_2-\varphi_i)+h, \theta_2\in[\varphi_i,\varphi_i+1/(2h)]\end{cases}, \quad (18)$$

where h is a variable to optimize the approximation and $2P_ih$ is the height of the peak. It is noted that the period of θ_2 is 2π. Additionally, the PDF of θ_2 is approximated as the sum of the functions related to all the taps:

$$\hat{p}(\theta_2)=\sum_{i=1}^{N_f} f_i(\theta_2), \int_{-\pi}^{\pi}\hat{p}(\theta_2)d\theta_2=\sum_{i=1}^{N_f}P_i=1. \quad (19)$$

As can be seen from (18) and (19), h is the only variable to minimize the approximation error of the approximate PDF in (19). For the numerically obtained PDFs in Figs. 2 through 5, the optimum value of h can be obtained by minimizing the approximation error:

$$h=\arg\min_{h\ge 1/(2\pi)}\int_{-\pi}^{\pi}\left|p(\theta_2)-\hat{p}(\theta_2)\right|d\theta_2, \quad (20)$$

where the absolute value of the difference between the exact and approximate PDFs is used to measure the accuracy of the approximation. Other approximation error metrics can also be adopted. The approximate distributions are plotted with the red line in Figs. 2 through 5, and the corresponding optimum values of h under all the scenarios are listed in Tables 1 through 3.

Table 1. Optimum variable values for $\beta_i=\beta$.

$\lvert\beta\rvert$	h
0.5	0.34
0.6	0.43
0.7	0.57
0.8	0.78
0.9	1.19

Table 2. Optimum variable values for equal power, $P_1=P_l=0.5$, $\varphi_1=-\pi/2$, and $\varphi_l=\pi/2$.

$\lvert\beta_1\rvert,\lvert\beta_l\rvert$	h
0.5, 0.5	0.22
0.6, 0.6	0.24
0.7, 0.7	0.26
0.8, 0.8	0.27
0.9, 0.9	0.38

Table 3. Optimum variable values for non-equal power, $\varphi_1=-\pi/2$ and $\varphi_l=\pi/2$.

$\lvert\beta_1\rvert,\lvert\beta_l\rvert$	h	
	$P_1=0.6, P_l=0.4$	$P_1=0.7, P_l=0.3$
0.5, 0.5	0.22	0.23
0.6, 0.6	0.24	0.25
0.7, 0.7	0.26	0.27
0.8, 0.8	0.27	0.29
0.9, 0.9	0.37	0.49

V. Adaptive Codebook Design for WBP

The adaptive nonuniform codebook for narrowband MIMO

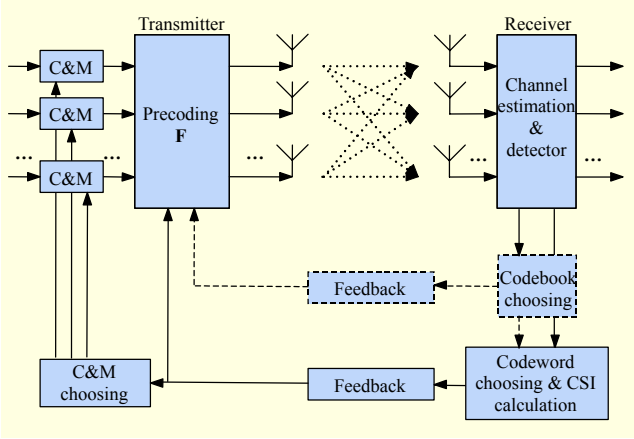

Fig. 6. Adaptive codebook in the MIMO-OFDM system.

systems is proposed in [14]. The spatial correlation coefficient is calculated according to the average at the receiver over a long period of time and sent back to the transmitter. Then, the current codebook is chosen. The use of the adaptive nonuniform codebook in the MIMO-OFDM system is illustrated in Fig. 6, where the codebook is adaptive to the correlation coefficients of the multi-path channel. Compared with Fig. 1, a new feedback link from the receiver to transmitter is used for the current codebook index. The feedback period of the codebook index is much longer than that of the codeword index. Hence, the system overhead increase due to the new feedback link is acceptable.

In the adaptive codebook design, θ_1 is fixed as $\pi/4$; hence, a codebook is equivalent to a quantization of θ_2. According to the approximate precoder distribution in subsection IV.2, adaptive quantization of θ_2 can be easily implemented. Let c_i be the i-th precoder (codeword) in codebook $\mathcal{C}$, which comprises M precoders. The distance between angles is defined as

$$d(\psi_1,\psi_2)=\min_{k\in Z}\left|\psi_1-\psi_2+2\pi k\right|. \tag{21}$$

For codebook $\mathcal{C}$, the quantized angle of θ_2 is obtained through minimizing (21) as

$$\hat{\theta}_2=\arg\min_{c_i\in C} d(\theta_2,c_i), \tag{22}$$

which is the codeword selection in the codebook. The quantization error is $d(\theta_2,\hat{\theta}_2)$. The codebook design problem with the approximate precoder distribution is equivalent to the average quantization error minimization problem below:

$$\mathcal{C}=\arg\min_{\mathcal{C}} E[d(\theta_2,\hat{\theta}_2)]. \tag{23}$$

The adaptive nonuniform codebook designs for two classic scenarios are taken as examples to explain the use of adaptive codebook design based on the approximate precoder distribution in subsection IV.2.

1. PDF with a Single Peak

If there is only a single peak in the envelope of the precoder distribution, that is, $\beta_i=\beta$, the symmetrical axis of $p(\theta_2)$ is $\theta_2=\varphi=\text{angle}(\beta)$, as shown in Fig. 2. According to (18) and (19), the approximate precoder distribution is given by

$$\hat{p}(\theta_2)=\begin{cases}4h^2(\theta_2-\varphi_i)+2h, \theta_2\in[\varphi-1/(2h),\varphi]\\ -4h^2(\theta_2-\varphi_i)+2h, \theta_2\in[\varphi,\varphi+1/(2h)]\end{cases}. \tag{24}$$

If M=2, the quantization of θ_2 is also symmetrical around φ and the codebook is represented by $\mathcal{C}_2=\{\varphi-t, \varphi+t\}$. As the precoder distribution and the codebook are both insensitive to angle rotation, we can assume that φ=0. Based upon this knowledge, the quantization error becomes a function of t as

$$R(t)=E\left[d(\theta_2,\hat{\theta}_2)\right]=-\frac{8}{3}h^2t^3+4ht^2-t+\frac{1}{6h}. \tag{25}$$

The optimum value of t can be obtained as

$$t=\arg\min_t R(t)=\frac{2-\sqrt{2}}{4h}. \tag{26}$$

The blue dashed line in Fig. 2 shows $\mathcal{C}_2$ obtained with (26). As can be seen from (26), the distance between the quantization orders and the symmetrical axis is related to h, and the product of h and t is constant.

For M=4, the codebook is denoted by $\mathcal{C}_4=\{\varphi-t_2, \varphi-t_1, \varphi+t_1, \varphi+t_2\}$. The quantization error becomes

$$\begin{aligned}R(t_1,t_2)=&-\frac{7}{3}h^2{t_1}^3-\frac{7}{3}h^2{t_2}^3+h^2t_1^2t_2+h^2t_1{t_2}^2\\&+3ht_1^2+3ht_2^2-2ht_1t_2-t_2+\frac{1}{6h}.\end{aligned} \tag{27}$$

The optimization problem can be solved with an exhaustive search in the interval of [0, 1/(2h)] as

$$(t_1,t_2)=\arg\min_{(t_1,t_2),0<t_1<t_2<1/(2h)} R(t)=(0.08h^{-1},0.27h^{-1}). \tag{28}$$

Figure 2 also plots $\mathcal{C}_4$, represented by the pink dashed line.

2. PDF with Multiple Peaks

For the scenario of $P_1=P_l=0.5$, $\varphi_1=-\pi/2$, and $\varphi_l=\pi/2$, the design of $\mathcal{C}_2$ is straightforward, that is, $\mathcal{C}_2=\{\varphi_1, \varphi_l\}$. If M=4 and the two peaks of the precoder distribution do not overlap as shown in Fig. 3(e), that is, $h>1/\pi$, the proposed codebook design in subsection V.1 for M=2 can be directly extended to

$$\mathcal{C}_4=\{\pm\pi/2\pm(2-\sqrt{2})/(4h)\}. \tag{29}$$

If the two peaks of the precoder distribution overlap as

shown in Figs. 3(a) to 3(d), the codebook can be obtained as $\mathcal{C}_4 = \{\pm\pi/2 \pm t\}$. The quantization error function contains t as a variable. If

$$t < \pi - \frac{1}{2h}, \tag{30}$$

then

$$R(t) = -\frac{4}{3}h^2t^3 + 2ht^2 - \frac{1}{2}t + \cdots, \tag{31}$$

where the constant independent of t is ignored. The quantization error is minimized as follows:

$$t = \arg\min_t R(t) = \frac{2-\sqrt{2}}{4h}. \tag{32}$$

Integrating (32) into (30) gives rise to the necessary condition of the codebook design in (30) as

$$h > \frac{4-\sqrt{2}}{4\pi}. \tag{33}$$

On the other hand, if

$$t > \pi - \frac{1}{2h}, \tag{34}$$

then

$$R(t) = (4h - 4h^2\pi)t^2 + \left(4\pi^2h^2 - 4\pi h + \frac{1}{2}\right)t + \cdots, \tag{35}$$

where the constant independent of t is ignored. The quantization error is minimized when

$$t = \frac{8\pi h - 1 - 8\pi^2h^2}{16h - 16h^2\pi}. \tag{36}$$

Substituting (36) into (34) gives rise to the necessary condition of the codebook design in (34) as

$$h < \frac{4-\sqrt{2}}{4\pi}. \tag{37}$$

Combining (32), (33), (36), and (37), the codebook design for the two-peak precoder distribution function can be summarized as

$$\mathcal{C}_4 = \begin{cases} \left\{\pm\frac{\pi}{2} \pm \frac{2-\sqrt{2}}{4h}\right\}, & \frac{4-\sqrt{2}}{4\pi} \le h < \frac{1}{\pi} \\ \left\{\pm\frac{\pi}{2} \pm \frac{8\pi h - 1 - 8\pi^2h^2}{16h - 16h^2\pi}\right\}, & \frac{1}{2\pi} < h < \frac{4-\sqrt{2}}{4\pi} \end{cases}. \tag{38}$$

As can be seen from (29) and (38), the codebook design for $h \ge (4-\sqrt{2})/(4\pi)$ is identical.

VI. Simulation Results

The system performance of the proposed adaptive nonuniform codebook for WBP is evaluated in this section, where the conventional fixed uniform codebook is taken as a comparative baseline scheme. The proposed adaptive nonuniform codebook is adaptive quantization of the precoder and related to the correlation coefficients of all the channel taps. Therefore, apparent reduction on the quantization error at the expense of a slight increase of the feedback overhead can be achieved with the proposed adaptive codebook.

The MIMO-OFDM system with WBP and the adaptive codebook is evaluated with the system parameters listed in Table 4. The ergodic capacity and BER are adopted as two performance metrics. The system ergodic capacity is defined as

$$C_a = \frac{1}{N_C}\sum_{n=1}^{N_C} E\left[\log_2(1+\gamma_n)\right], \tag{39}$$

where γ_n is the post signal-to-noise ratio (SNR) over the n-th subcarrier after maximum ratio combining (MRC).

In our simulations, each channel tap is generated with an i.i.d. channel matrix and the correlation coefficient according to (13) and (14) in [14]. According to (5), the channel matrices of all the subcarriers can be obtained. Then, the optimum precoder is computed with (10), and the corresponding angle θ_2 is achieved with (17). The quantized angle $\hat{\theta}_2$, that is, the precoder in the codebook, is selected with (22). The post SNR over each subcarrier can be computed with the selected precoder and $\mathbf{H}_n$. The two-tap channel in section IV is also adopted in this part, and l=4.

1. Equal Power and Correlation Coefficient for All Taps

Assume P_1=P_l=0.5 and β=0.5$e^{j\pi/2}$. Two adaptive codebooks

Table 4. System parameters for performance evaluation.

Sampling frequency ($1/\Delta t$)	960 kHz
DFT size (N)	64
Number of available subcarriers	64
OFDM symbol duration	Data: 66.67 μs CP: 4.56 μs
Length of subframe	1 ms (14 OFDM symbols)
$N_T \times N_R$	2×2
Mobile speed	3 km/h
Modulation	Binary phase-shift keying
Receiver algorithm	MRC

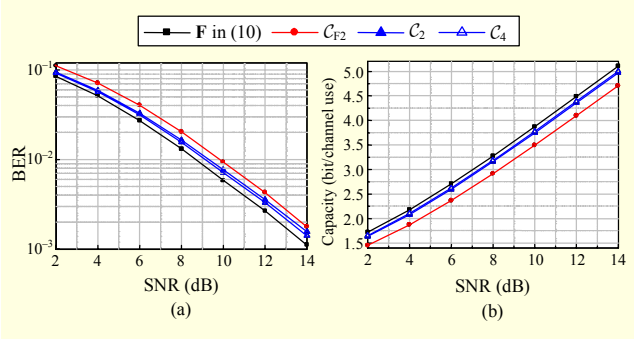

Fig. 7. (a) BER performance and (b) capacity performance for β=0.5e$^{j\pi/2}$.

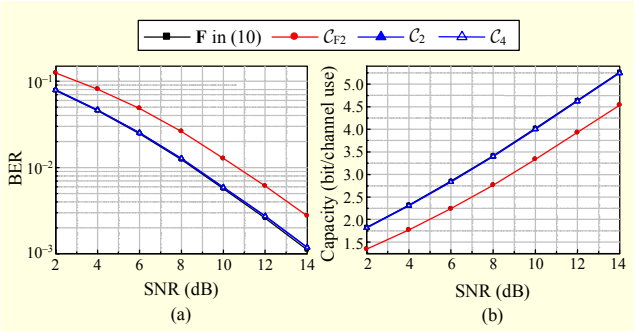

Fig. 8. (a) BER performance and (b) capacity performance for β=0.9e$^{j\pi/2}$.

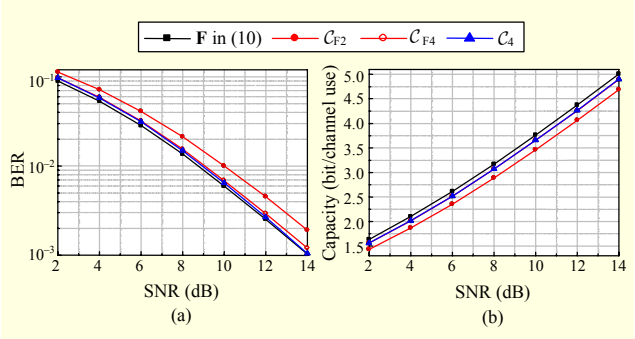

Fig. 9. (a) BER performance and (b) capacity performance for β_1=0.6e$^{-j\pi/2}$ and β_f=0.6e$^{j\pi/2}$.

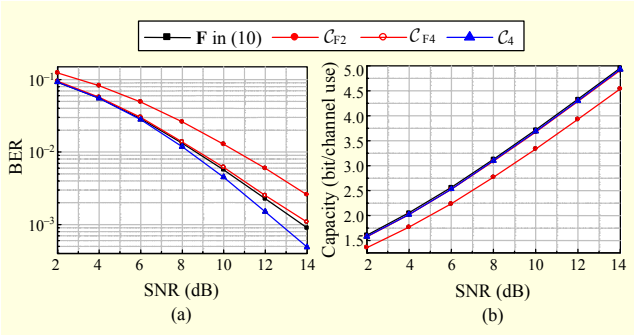

Fig. 10. (a) BER performance and (b) capacity performance for β_1=0.9e$^{-j\pi/2}$ and β_f=0.9e$^{j\pi/2}$.

Table 5. SNR gains in dB over $\mathcal{C}_{F2}$ for equal correlation coefficient (BER=10^{-2}, C_a=3.0 bits/channel use).

	β	BER	Capacity
$\mathcal{C}_2$	0.5e$^{j\pi/2}$	0.51	0.88
	0.9e$^{j\pi/2}$	2.07	2.26
$\mathcal{C}_4$	0.5e$^{j\pi/2}$	0.67	0.96
	0.9e$^{j\pi/2}$	2.07	2.26

are constructed according to subsection V.1: 1) $\mathcal{C}_2$={1.14, 2.00} and 2) $\mathcal{C}_4$={0.78, 1.34, 1.81, 2.36}. The fixed uniform quantization codebook ($\mathcal{C}_{F2}$={0, π}) is also taken for comparison. Additionally, the results based on (10) are plotted in the figures, which are equivalent to a codebook with an infinite size.

The BER and capacity results are given in Fig. 7. Obviously, the precoder in (10) performs the best without quantization errors. The adaptive nonuniform codebook, $\mathcal{C}_2$, outperforms the fixed one, $\mathcal{C}_{F2}$, by about 0.6 dB in the BER and 0.9 dB in capacity, as shown in Figs. 7(a) and 7(b), respectively. The difference between $\mathcal{C}_2$ and $\mathcal{C}_4$ is less than 0.2 dB.

The performance with β=0.9e$^{j\pi/2}$ is also evaluated, where $\mathcal{C}_2$={1.45, 1.69} and $\mathcal{C}_4$={1.34, 1.50, 1.64, 1.80}. The results are given in Fig. 8. As can be observed from Fig. 2(e), $p(\theta_2)$ is close to $\varphi=\pi/2$, so that precoding based on $\mathcal{C}_2$ and $\mathcal{C}_4$ performs almost the same as the noncodebook precoder. The feedback overhead can be extremely reduced without obvious performance loss in this scenario.

The SNR gains in dB of $\mathcal{C}_2$ and $\mathcal{C}_4$ over $\mathcal{C}_{F2}$ in Figs. 7 and 8 are listed in Table 5. The improvement in the capacity with the proposed adaptive codebook over the conventional fixed codebook is more apparent than that in the BER.

2. Equal Power and Different Spatial Correlations

Various tap correlation coefficients are considered in this scenario. The BER and capacity results for P_1=P_f=0.5, β_1=0.6e$^{-j\pi/2}$, and β_f=0.6e$^{j\pi/2}$ are shown in Fig. 9. The fixed codebook $\mathcal{C}_{F4}=\{\pm\pi/4, \pm 3\pi/4\}$ is included for comparison. According to (37), we have $\mathcal{C}_4=\{\pm 0.96, \pm 2.18\}$. The performance of $\mathcal{C}_{F2}$ is far from the performances of the other schemes. As shown in Fig. 9(a), $\mathcal{C}_4$ performs closely to $\mathcal{C}_{F4}$ at the low SNR region and outperforms it at high SNRs.

For β_1=0.9e$^{-j\pi/2}$ and β_f=0.9e$^{j\pi/2}$, the BER and capacity results are plotted in Fig. 10, where $\mathcal{C}_4=\{\pm 1.19, \pm 1.96\}$ is in

Table 6. SNR gains in dB over $\mathcal{C}_{F2}$ and $\mathcal{C}_{F4}$ for different correlation coefficient (BER=10^{-2}, C_a=3.0 bits/channel use).

	β_1, β_l	BER	Capacity
$\mathcal{C}_{F2}$	$0.6e^{-j\pi/2}$, $0.6e^{j\pi/2}$	1.02	0.63
	$0.9e^{-j\pi/2}$, $0.9e^{j\pi/2}$	2.31	1.14
$\mathcal{C}_{F4}$	$0.6e^{-j\pi/2}$, $0.6e^{j\pi/2}$	0.10	0
	$0.9e^{-j\pi/2}$, $0.9e^{j\pi/2}$	0.48	0

accordance with (29). The capacity results with $\mathcal{C}_{F4}$, $\mathcal{C}_4$, and the noncodebook precoding are similar. However, $\mathcal{C}_4$ outperforms $\mathcal{C}_{F4}$ by about 1.4 dB in terms of BER, as shown in Fig. 10(a).

Similarly, the results in Figs. 9 and 10 are summarized in Table 6. For the channels with different correlation coefficients, the proposed adaptive nonuniform codebook is capable of reducing quantization errors and improving on the system reliability and capacity. The SNR gains at the same levels of the BER are more apparent than those in capacity, which is different from the observation in Table 5. The results in Tables 5 and 6 clearly demonstrate the advantage of the proposed adaptive codebook over the conventional codebook.

VII. Conclusion

In this paper, we studied the precoder distribution with WBP under the spatially correlated channel, which was shown to be related to the average power and spatial correlation coefficient of each channel tap. Then, a unified approximate expression of the precoder distribution function was proposed, where the PDF related to each tap was approximated by an isosceles triangle and the precoder distribution was approximated by the overlapped functions of all the taps. Based on the proposed approximation, an adaptive nonuniform codebook design for WBP was presented. The BER and capacity performances obtained via Monte Carlo simulations clearly demonstrated the advantage of the proposed adaptive codebook.

References

[1] G.J. Foschini and M.J. Gans, "On Limits of Wireless Communications in a Fading Environment When Using Multiple Antennas," *Wireless Personal Commun.*, vol. 6, no. 3, Mar. 1998, pp. 311-335.

[2] 3GPP TS 36.211 v8.8.0, "Physical Channels and Modulation," Sept. 2009. Available at: http://www.3gpp.org/ftp

[3] IEEE P802.11n/D1.04, "Wireless LAN Medium Access Control (MAC) and Physical Layer (PHY) Specifications: Enhancements for Higher Throughput," Sept. 2006.

[4] S. Liu and J.-W. Chong, "Improved Design Criterion for Space-Frequency Trellis Codes over MIMO-OFDM Systems," *ETRI J.*, vol. 26, no. 6, Dec. 2004, pp. 622-634.

[5] A. Scaglione, S. Barbarossa, and G.B. Giannakis, "Filterbank Transceivers Optimizing Information Rate in Block Transmissions over Dispersive Channels," *IEEE Trans. Inf. Theory*, vol. 45, no. 3, Apr. 1999, pp. 1019-1032.

[6] K.J. Kim, M.O. Pun, and R.A. Iltis, "QRD-Based Precoded MIMO-OFDM Systems with Reduced Feedback," *IEEE Trans. Comm.*, vol. 58, no. 2, Feb. 2010, pp. 394-398.

[7] K.J. Kim, M.O. Pun, and R.A. Iltis, "QRD-Based Precoded MIMO-OFDM Systems with Reduced Feedback," *Proc. IEEE ICC*, Beijing, China, May 2008, pp. 708-712.

[8] H. Long et al., "Improved Wideband Precoding with Arbitrary Sub-Carrier Grouping in MIMO-OFDM Systems," *ETRI J.*, vol. 34, no. 1, Feb. 2012, pp. 9-16.

[9] K.J. Kim et al., "A Reduced Feedback Precoder for MIMO-OFDM Cooperative Diversity Systems," *IEEE Trans. Veh. Technol.*, vol. 61, no. 2, Feb. 2012, pp. 584-596.

[10] J.C. Roh and B.D. Rao, "Transmit Beamforming in Multiple-Antenna Systems with Finite Rate Feedback: A VQ-Based Approach," *IEEE Trans. Inf. Theory*, vol. 52, no. 3, Mar. 2006, pp. 1101-1112.

[11] D.J. Love, R.W. Heath, Jr., and T. Strohmer, "Grassmannian Beamforming for Multiple-Input Multiple-Output Wireless Systems," *IEEE Trans. Inf. Theory*, vol. 49, no. 10, Oct. 2003, pp. 2735-2747.

[12] D.J. Love and R.W. Heath, Jr., "Limited Feedback Precoding for Spatial Multiplexing Systems," *Proc. IEEE Globecom*, vol. 4, San Francisco, CA, USA, Dec. 2003, pp. 1857-1861.

[13] A.T. James, "Distributions of Matrix Variates and Latent Roots Derived from Normal Samples," *Annals Math. Statistics*, vol. 35, June 1964, pp. 475-501.

[14] H. Long et al., "Precoding Vector Distribution under Spatial Correlated Channel and Nonuniform Codebook Design," *Proc. IEEE ICC*, Beijing, China, May 2008, pp. 4506-4510.

[15] Y. Fu, C. Tellambura, and W.A. Krzymien, "Limited-Feedback Precoding for Closed-Loop Multiuser MIMO OFDM Systems with Frequency Offset," *IEEE Trans. Wireless Commun.*, vol. 7, no. 11, Nov. 2008, pp. 4155-4165.

Hang Long received his BS and PhD from Beijing University of Posts and Telecommunications (BUPT), Beijing, China, in 2005 and 2010, respectively. Since 2010, he has been with BUPT as a postdoctoral researcher. His current research interests are in the field of signal processing for wireless communications with emphasis on MIMO and cooperative communications.

Kyeong Jin Kim received his MS from the Korea Advanced Institute of Science and Technology (KAIST), Daejeon, Rep. of Korea, in 1991 and his PhD in electrical and computer engineering from the University of California, Santa Barbara, Santa Barbara, CA, USA, in 2000. From 1991 to 1995, he was a research engineer at the Video Research Center of Daewoo Electronics Ltd., Rep. of Korea. In 1997, he joined the Data Transmission and Networking Laboratory at the University of California, Santa Barbara, USA. After receiving his degrees, he joined the Nokia Research Center in Dallas as a senior research engineer. From 2005 to 2009, he worked with the Nokia Corporation in Dallas, TX, USA, as an L1 specialist. From 2010 to 2012, he was a professor by invitation for Inha University, Incheon, Rep. of Korea. Currently, he is working as a member of the senior principal research staff at Mitsubishi Electric Research Laboratories (MERL), Cambridge, MA, USA. His research has focused on transceiver design, resource management, and scheduling in the wireless communication systems. He serves as an editor for IEEE Communications Letters.

Wei Xiang received his BEng and MEng, both in electronic engineering, from the University of Electronic Science and Technology of China, Chengdu, China, in 1997 and 2000, respectively, and his PhD in telecommunications engineering from the University of South Australia, Adelaide, Australia, in 2004. In January 2004, he joined the Faculty of Engineering and Surveying, University of Southern Queensland, Toowoomba, Australia, where he was first an associate lecturer in the Department of Computer Systems Engineering from 2004 to 2006, then a lecturer from 2007 to 2008, and currently holds a faculty post as a senior lecturer. In 2008, he was a visiting scholar at the School of Electrical and Electronic Engineering, Nanyang Technological University, Singapore. From October 2010 to March 2011, he was a visiting scholar at the University of Mississippi, Oxford, MS, USA. He was awarded a prestigious Queensland International Fellowship in 2010. He received the Best Paper Award at the 2011 IEEE WCNC. Most recently, he was awarded an extremely competitive three-year Smart Futures Fellowship by the Queensland Government of Commonwealth Australia for the period of 2012 to 2015 and an internationally prestigious Endeavour Research Fellowship by the Australian Government. As such, he was recently appointed by the University of Hong Kong as a visiting associate professor for the period of September 2012 to March 2013 to undertake his Endeavour Research Fellowship project. His research interests are in the broad area of communications and information theory, particularly coding and signal processing for multimedia communications systems.

Jing Wang received her BS from Beijing University of Posts and Telecommunications (BUPT), Beijing, China, in 2011. Since 2011, she has been working toward her MS at BUPT. Her current research interests are in the field of wireless physical layer techniques.

Yuanan Liu received his BS, MS, and PhD from the University of Electronic Science and Technology of China, Chengdu, China, in 1984, 1989, and 1992, respectively. He is currently a professor at and the dean of the School of Electronic Engineering, Beijing University of Posts and Telecommunications (BUPT), Beijing, China. His research interests include mobile communications and electromagnetic compatibility.

Wenbo Wang received his BS, MS, and PhD from Beijing University of Posts and Telecommunications (BUPT), Beijing, China, in 1986, 1989, and 1992, respectively. He is currently a professor at and the dean of the Graduate School, BUPT. His research interests include signal processing, mobile communications, and wireless ad hoc networks.